Nodal signalling is involved in left–right asymmetry in snails

Cristina Grande[1,2,3] & Nipam H. Patel[1,2,3]

Many animals display specific internal or external features with left–right asymmetry. In vertebrates, the molecular pathway that leads to this asymmetry uses the signalling molecule Nodal, a member of the transforming growth factor-β superfamily[1], which is expressed in the left lateral plate mesoderm[2], and loss of *nodal* function produces a randomization of the left–right asymmetry of visceral organs[3,4]. Orthologues of *nodal* have also been described in other deuterostomes, including ascidians and sea urchins[5,6], but no *nodal* orthologue has been reported in the other two main clades of Bilateria: Ecdysozoa (including flies and nematodes) and Lophotrochozoa (including snails and annelids). Here we report the first evidence for a *nodal* orthologue in a non-deuterostome group. We isolated *nodal* and *Pitx* (one of the targets of Nodal signalling) in two species of snails and found that the side of the embryo that expresses *nodal* and *Pitx* is related to body chirality: both genes are expressed on the right side of the embryo in the dextral (right-handed) species *Lottia gigantea* and on the left side in the sinistral (left-handed) species *Biomphalaria glabrata*. We pharmacologically inhibited the Nodal pathway and found that *nodal* acts upstream of *Pitx,* and that some treated animals developed with a loss of shell chirality. These results indicate that the involvement of the Nodal pathway in left–right asymmetry might have been an ancestral feature of the Bilateria.

Asymmetric expression and action of the Nodal pathway is a conserved feature of deuterostomes, with *nodal* and its target gene *Pitx* acting on the left side of the embryo in chordates but on the right side in echinoderms (sea urchins)[7]. Until now, the lack of identified *nodal* orthologues in the genomes of cnidarians and ecdysozoans suggested that *nodal* evolved in an ancestor within the early deuterostome lineage. Furthermore, although the molecular pathways involved in several asymmetries in flies and nematodes are being actively investigated, so far the Nodal pathway does not seem to be involved. The third main group of Bilateria, the Lophotrochozoa, which includes snails and annelids, also displays morphological asymmetries. One of the asymmetries that has particularly intrigued researchers is snail chirality, which refers to the body handedness and direction of shell coiling (Fig. 1). Dextral (right-handed) and sinistral (left-handed) forms can be found at many taxonomic levels (Fig. 1a, b), although most extant snail species are dextral[8]. Body chirality can be related to a much earlier chirality that is seen in all gastropod embryos, namely the chirality of the spiral cleavage pattern seen at the transition from the 4- to 8-cell embryo (Fig. 1c). For some species, both chiral forms exist within a population (Fig. 1b), and body handedness is determined by a single locus that functions maternally to determine the chirality of offspring[9–11].

To gain insight into the molecular pathway for left–right asymmetry in gastropods, we investigated some of the previously described genes critical for left–right determination in other organisms. Specifically, we focused on members of the Nodal pathway in two species of snails that differ in chirality: the sinistral species

Biomphalaria glabrata (Fig. 1d), an intermediate host for the pathogen that causes schistosomiasis, and the dextral species *Lottia gigantea* (Fig. 1e), the complete genome sequence of which has been assembled. We first found in *L. gigantea* several components of the Nodal signalling pathway, including *nodal* itself as well as one of the known target genes of *nodal*, the paired homeobox gene *Pitx*. We subsequently characterized complementary DNAs encoding proteins
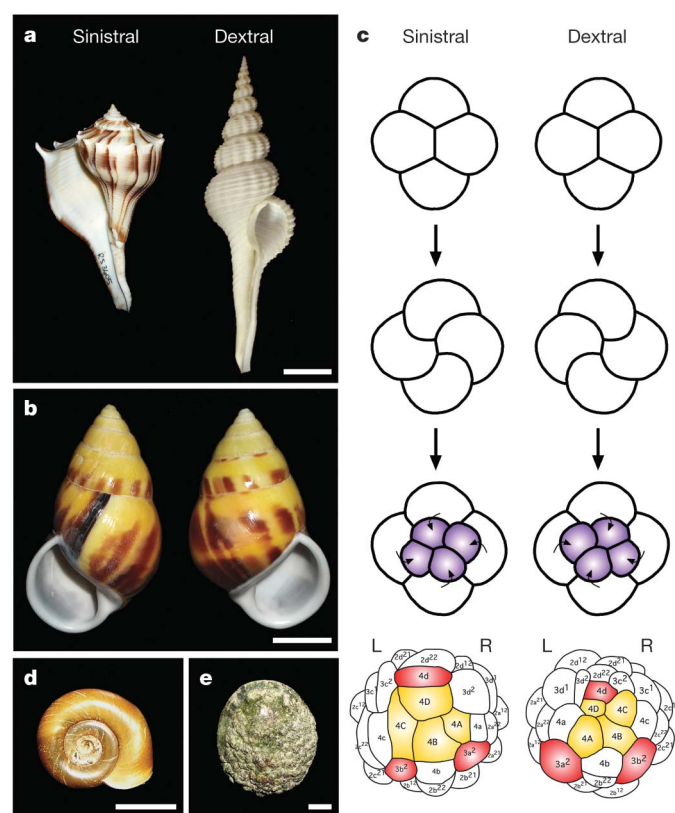

Figure 1 | Chirality in snails. a, Species with different chirality: sinistral *Busycon pulleyi* (left) and dextral *Fusinus salisbury* (right). **b,** Sinistral (left) and dextral (right) shells of *Amphidromus perversus*, a species with chiral dimorphism. **c,** Early cleavage in dextral and sinistral species (based on ref. 27). In sinistral species, the third cleavage is in a counterclockwise direction, but is clockwise in dextral species. In the next divisions the four quadrants (A, B, C and D) are oriented as indicated. Cells coloured in yellow have an endodermal fate and those in red have an endomesodermal fate in *P. vulgata*[15] (dextral) and *B. glabrata* (sinistral)[28]. L and R indicate left and right sides, respectively. **d,** *B. glabrata* possesses a sinistral shell and sinistral cleavage and internal organ organization. **e,** *L. gigantea* displays a dextral cleavage pattern and internal organ organization, and a relatively flat shell characteristic of limpets. Scale bars: **a,** 2.0 cm; **b,** 1.0 cm; **d,** 0.5 cm; **e,** 1.0 cm.

[1]Department of Molecular and Cell Biology, [2]Department of Integrative Biology, and [3]Center for Integrative Genomics, University of California, Berkeley, California 94720-3200, USA.

related to Nodal and Pitx in both *L. gigantea* and *B. glabrata*. Bayesian phylogenetic analyses confirmed, with high statistical support, that these potential orthologues of Nodal are indeed more closely related to deuterostome Nodal than to any other transforming growth factor-β (TGF-β) family member (Supplementary Figs 1a and 2). To determine whether *nodal* is also present in other lophotrochozoans, we also identified a potential orthologue of *nodal* in the annelid *Capitella* species I, and further phylogenetic analyses confirmed the close relationship between this sequence and those of the gastropod and deuterostome Nodal proteins (Supplementary Figs 1a and 2). In addition, a single potential orthologue of *Pitx* was identified in both snail species (Supplementary Fig. 1b).

We then examined the expression pattern of *nodal* and *Pitx* in both *L. gigantea* and *B. glabrata*. Snail embryos undergo indirect development, producing first a trochophore and then a veliger larva. We first examined the trochophore stage because the anterior–posterior and dorsal–ventral axes at this time are morphologically clear, and found that both genes were expressed in left–right asymmetric patterns (Fig. 2). In *L. gigantea* there are two ectodermal domains of *nodal* expression on the right side of the embryo: one cephalic region plus a lateral domain near where shell formation initiates (Fig. 2a–d). In *B. glabrata*, expression is seen in an ectodermal region on the left side of the embryo near where the shell gland will form in the posterior midline region (Fig. 2e–h). In the veliger stage of *B. glabrata*, an additional domain in the left cephalic ectoderm is seen (Supplementary Fig. 3). To confirm the right versus left expression, we double-labelled embryos of both species for *nodal* and *hedgehog*, a gene that is expressed at the ventral midline in snails (Fig. 2i–l)[12].

At the trochophore stage of *L. gigantea*, *Pitx* expression is seen in a group of ectodermal cells on the right side of the larvae, adjacent to those that express *nodal*, as well as in the developing gut (Figs 2m, n and 3i, j). At later stages, *Pitx* expression is maintained in these domains but also becomes visible in the right cephalic ectoderm and in a symmetric domain of the visceral mass (Supplementary Fig. 4). In the trochophore of *B. glabrata*, *Pitx* expression is observed in the ectoderm on the left side of the larvae close to the shell gland and adjacent to the group of cells that express *nodal*, as well as in symmetric patterns in the stomodeum and gut (Fig. 2o–p). Later in development, *Pitx* is also symmetrically expressed in the developing cephalic tentacles (Supplementary Fig. 4).

We next examined earlier stages of development to determine when the asymmetric patterns were first visible. In both species, *nodal* transcripts were first detected at the 32-cell stage (Fig. 3a, c). The bilateral axis is visible in snails at the 32- to 64-cell stage, when the macromere of the D quadrant, 3D, produces mesentoblast 4d, which subsequently divides in a bilateral fashion to form paired stem cells that will give rise to the mesodermal germ bands[13]. Embryos of *L. gigantea* double-labelled for *nodal* and *brachyury*, a gene that is expressed in 3D, mesentoblast 4d and then very strongly in the distinctly left–right bilateral cells 3d^2 and 3c^2 (ref. 14), show that the expression of *nodal* is clearly left–right asymmetric at the 32–64-cell stage and beyond (Fig. 3e–h). Using the *P. vulgata* fate map[15] as a guide, we conclude that *nodal* is expressed in the C quadrant, specifically in the derivatives of the micromeres 1c and 2c. In *P. vulgata*, the progeny of 1c are part of the right cephalic ectoderm of the larvae, whereas 2c-derived cells are part of the ectoderm of the right side of the foot, the mantle fold and the shell field[15], suggesting that the two ectodermal domains seen at the larval stages are composed of a subset of the nodal-expressing cells from the 64-cell stage. *Pitx* expression was first detected in both snail species at the 64-cell stage in a group of cells of the D quadrant, close to those that express *nodal* (Fig. 3b, d, i and j).

To investigate the function of Nodal signalling in snail development experimentally, we used the chemical inhibitor SB-431542. The TGF-β superfamily includes a large number of ligands but, because the drug SB-431542 specifically interferes with type I receptors Activin receptor-like kinase 4 (Alk4), Alk5 and Alk7 (ref. 16), only the activity of
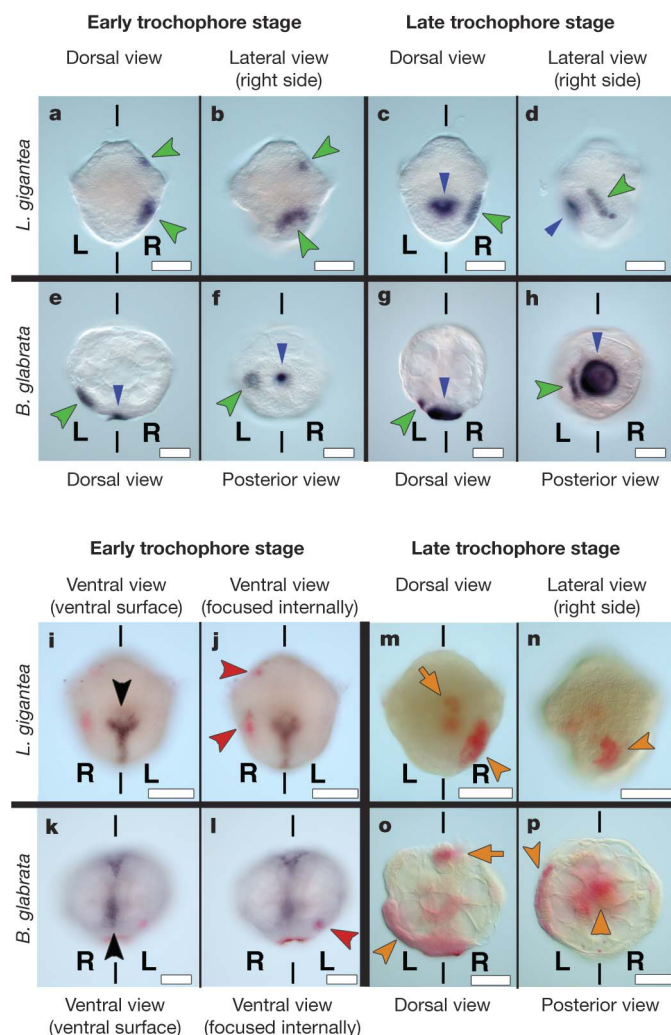

Figure 2 | *nodal* and *Pitx* expression in snails. Anterior is up, L and R indicate left and right sides. The blue arrowhead in **c–h** indicates non-specific staining of the shell. **a, b,** *nodal* is expressed in the right cephalic region (upper green arrowhead) and in the right lateral ectoderm (lower green arrowhead) in *L. gigantea*, as seen from dorsal (**a**) and right lateral (**b**) views. **c,** Expression is maintained in the right lateral ectoderm (green arrowhead); the right lateral view (**d**) shows that *nodal* expression (green arrowhead) is near the right side of the developing shell (blue arrowhead). **e–h,** *nodal* is expressed in the left lateral ectoderm (green arrowhead) in *B. glabrata*, as seen from dorsal (**e**) and posterior (**f**) views; **g, h,** Expression is maintained in the left lateral ectoderm (green arrowhead); the posterior view (**h**) shows that *nodal* expression (green arrowhead) is near the left side of the developing shell (blue arrowhead). **i–l,** *hedgehog* (black arrowheads in **i** and **k**) is expressed along the ventral midline, and *nodal* (red arrowheads in **j** and **l**) is expressed on the right side of *L. gigantea* (**j**) and on the left side of *B. glabrata* (**l**). **m, n,** *Pitx* is expressed in the visceral mass (orange arrow) and right lateral ectoderm (orange arrowhead) in *L. gigantea*, as seen from dorsal (**m**) and right lateral (**n**) views. **o, p,** *Pitx* is expressed in the stomodeum (orange arrow), visceral mass (orange triangle) and the left lateral ectoderm (orange arrowhead) in *B. glabrata*, as seen from dorsal (**o**) and posterior (**p**) views. Scale bars: 50 μm.

Nodal, Activin and TGF-β subfamily ligands are expected to be blocked by this drug. Of the potential members of the TGF-β superfamily that we have identified in the genome of *L. gigantea* (Supplementary Results and Supplementary Fig. 2), only Nodal and Activin signalling should be affected by SB-431542. Given, however, that we have not been able to detect the expression of any of the potential *activin* homologues during embryonic or larval stages, we suggest that SB-431542 treatment might affect Nodal signalling exclusively during snail development before the juvenile stage.
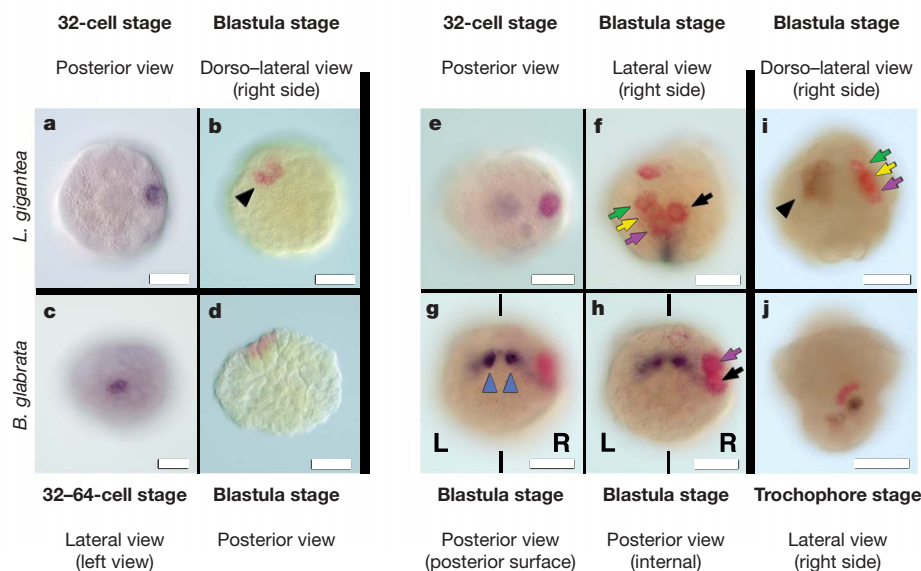
Figure 3 | Early expression of *nodal* and *Pitx* in snails. a, 32-cell stage *L. gigantea* expressing *nodal* in a single cell. **b**, Group of cells expressing *Pitx* in *L. gigantea*. **c**, Onset of *nodal* expression in *B. glabrata*. **d**, A group of cells expressing *Pitx* in *B. glabrata*. **e**, 32-cell *L. gigantea* expressing *nodal* (red) in a single cell (2c) and *brachyury* (black) in two cells (3D and 3c). **f–h**, *brachyury* (black) is expressed in a symmetrical manner in progeny of 3c and 3d blastomeres (blue triangles in **g**), thus marking the bilateral axis, and *nodal* (red) is expressed on the right side of *L. gigantea* in the progeny of 2c

and 1c blastomeres, as seen from the lateral (**f**) and posterior (**g**, **h**) views of the same embryo. **i**, A group of cells expressing *nodal* (red) in the C quadrant and *Pitx* (black) in the D quadrant of the 120-cell-stage embryo of *L. gigantea*. **j**, *nodal* (red) and *Pitx* (black) expression in adjacent areas of the right lateral ectoderm in *L. gigantea*. L and R indicate the left and right sides of the embryo, respectively. The black triangle in **b** and **i**, the green, yellow and pink arrows in **f** and **i**, and the black and pink arrows in **f** and **h** point to the equivalent cells. Scale bars: 50 μm.

Different developmental stages of *B. glabrata* were treated with SB-431542, and the percentages of specific abnormalities varied depending on the concentration and the timing of drug treatment (Supplementary Table 1). The most frequently observed phenotype after application of drug at early stages (1–16 cells) was the production of embryos that failed to complete gastrulation and thus could not form juveniles with shells. Some of the embryos that successfully completed gastrulation, however, displayed a striking phenotype– they developed with non-coiled shells (Fig. 4a–g). At 5 μM drug concentration, the straight-shelled phenotype was seen in 8% of the animals that managed to complete gastrulation, but at 10 μM concentration this value rose to 43% of those that completed gastrulation.

Although the shells showed a slight dorsal–ventral curvature, they were tubular with no sign of the left-handed coiling usually seen in *B. glabrata* (Fig. 4a–g). Varying the time of drug application revealed that exposure at the trochophore stage or later yielded animals that were almost always normal, and exposure at the blastula or gastrula stage yielded no coiling defects. Only by applying the drug before the blastula stage could we obtain animals with coiling defects, suggesting that a role in left–right asymmetry might be the earliest function of *nodal* within the embryo (see Supplementary Table 1). Efforts to further narrow the time of drug inhibition by washing off the drug were ineffective, possibly owing to the slow diffusion rate of the drug through the egg capsule or a slow reversal of the biochemical effect of the drug on the receptors.

We also followed the development of some of the animals with straight shells over the course of several days. We found that these animals continued to enlarge their shells, indeed forming shells that were quite long and robust, but remained straight (Supplementary Fig. 5). To rule out the possibility that the lack of shell coiling was simply due to general poor growth, we applied a different chemical
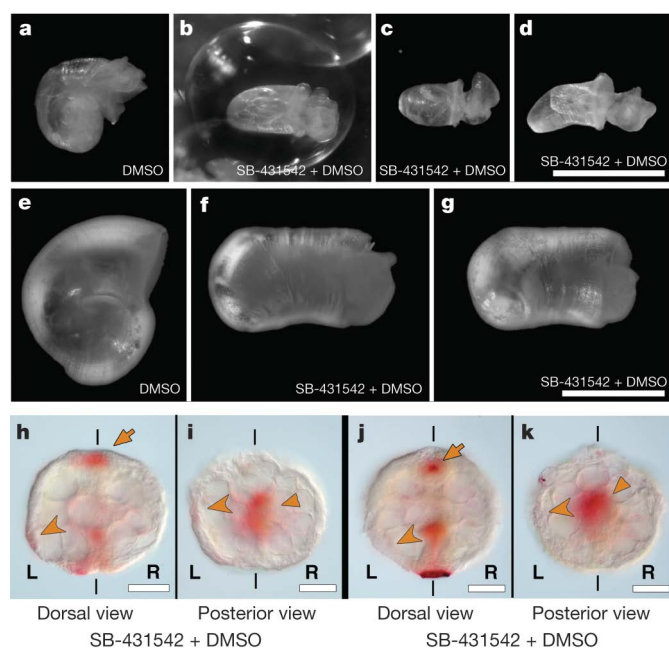

Figure 4 | Wild-type coiled and drug-treated non-coiled shells of *B. glabrata* and *Pitx* expression in drug-treated embryos. Control animals (**a**, **e**) display the normal sinistral shell morphology. Drug-treated animals (**b–d**, **f**, **g**, exposed to SB-431542 from the 2-cell stage onwards) have straight shells. **b–d** show three different living individuals; **f** and **g** are a fourth individual, ethanol-fixed, and shown from the side (**f**) and slightly rotated (**g**). **h–k**, *Pitx* expression in embryos exposed to SB-431542. Dorsal (**h**) and posterior (**i**) views of an embryo showing reduced levels of expression. *Pitx* expression is maintained in the stomodeum (orange arrow in **h**) and the visceral domain (orange triangle in **i**), but asymmetric expression in left ectoderm is greatly reduced (orange arrowhead). Dorsal (**j**) and posterior (**k**) views of an embryo in which the asymmetric ectodermal expression of *Pitx* is undetectable (orange arrowhead in **j** and **k** show where expression would be expected), although the stomodeal (orange arrow in **j**) and visceral (orange triangle in **k**) domain expression of *Pitx* is normal. *Pitx* expression levels shown in **h–k** should be compared to levels in wild-type embryos in Fig. 2o and p, which are the same levels seen in DMSO-treated animals. L and R indicate the left and right sides of the embryo, respectively. Scale bars: **a–d**, 1.0 mm; **e–g**, 0.5 mm; **h–k**, 50 μm.

inhibitor, rapamycin—a drug that interferes with the cellular metabolic machinery modifying cell growth and proliferation (see Methods Summary). Although the treated embryos showed various, sometimes severe, defects in their morphology, the shells that were formed always showed some degree of coiling. Non-coiled shells similar to those recovered with the SB-431542 drug treatment were not detected (Supplementary Table 2).

To test the effects of the SB-431542 drug treatment on the Nodal pathway at the molecular level, we compared the levels of expression of *nodal* and *Pitx* in control and drug-treated embryos. Although no variation in levels of *nodal* expression was detected (both control and drug-treated embryos that survived to the trochophore stage showed strong *nodal* expression), in 30% of the treated embryos the level of expression in the asymmetric domain of *Pitx* was greatly reduced (Fig. 4h, i and Supplementary Table 3) and in 9.5% of the treated embryos asymmetric expression was undetectable (Fig. 4j, k and Supplementary Table 3). Only the asymmetric expression of *Pitx* was affected by the drug treatment; expression levels in the symmetric domains in the stomodeum and gut were unaltered, suggesting separate regulatory elements for these domains of expression, as previously described in deuterostomes[17]. These results indicate that *Pitx* is downstream from *nodal* in snails, as in deuterostomes. However in snails, unlike in deuterostomes, *nodal* does not seem to regulate its own expression. This is consistent with our observation that *nodal* expression in snails is asymmetric from the outset, whereas in vertebrates *nodal* expression is initially symmetric and depends on the regulated feedback of *nodal* signalling to achieve an asymmetric pattern[2].

The drug treatment results, together with our analysis of the expression of *nodal* and *Pitx*, provide preliminary support for our contention that Nodal signalling has a role in left–right asymmetry in snails. The reduction of Nodal signalling leads to a randomization of asymmetry in vertebrates, but it is interesting to note that we observe a lack of asymmetry in snails. Although chirality in snails is first defined at the transition from the 4- to the 8-cell stage, the first indication of morphological asymmetry in snails is given by a displacement of the shell gland to the left in dextral species and to the right in sinistral species. We suggest that the asymmetric activity of the Nodal pathway could lead to unequal formation of shell-producing cells on the two sides of the embryo, or could asymmetrically alter the rate of shell production.

Our results provide new insights into the evolution of body plans and left–right specification in Bilateria. Previous studies suggest that some general mechanisms (at the level of involvement of gap junctions and $(H^+ + K^+)$ATPase activity) contributing to left–right asymmetry are shared between distant phyla[18,19]. We hypothesize that there is an even closer linkage. Although *Pitx* orthologues have also been identified in non-deuterostomes such as *Drosophila melanogaster* and *Caenorhabditis elegans*, in these species *Pitx* has not been reported in asymmetrical expression patterns. Our results suggest that asymmetrical expression of *Pitx* might be an ancestral feature of the bilaterians. Furthermore, our data suggest that *nodal* was present in the common ancestor of all bilaterians and that it too may have been expressed asymmetrically. Various lines of evidence indicate that the last common ancestor of all snails had a dextral body[20]. If this is true, then our data would suggest that this animal expressed both *nodal* and *Pitx* on the right side. Combined with the fact that *nodal* and *Pitx* are also expressed on the right side in sea urchins[7,21], this raises the possibility that the bilaterian ancestor had left–right asymmetry controlled by *nodal* and *Pitx* expressed on the right side of the body. Although independent co-option is always a possibility, the hypotheses we present can be tested by examining *nodal* and *Pitx* expression and function in a variety of additional invertebrates.

Our data also provide a molecular entry point into understanding chirality in snails. In vertebrates, the actual symmetry-breaking event occurs before *nodal* is asymmetrically expressed, and the mechanisms that break symmetry seem to be different between various vertebrate species[2,22–24]. Likewise, in snails symmetry must be broken before the 8-cell stage, before *nodal* expression begins. Chirality in snails is determined by a still uncharacterized maternal factor, but once chirality is established *nodal* and *Pitx* are expressed on one side of the embryo. Future studies that determine how *nodal* expression is regulated will lead us towards an understanding of the actual symmetry-breaking event in snails, and examination of the steps downstream of Nodal signalling will provide new insights into the developmental control of complex animal morphologies such as shell coiling.

METHODS SUMMARY

We searched the National Center for Biotechnology Information (NCBI) database of genomic sequences from *L. gigantea*, and found nine potential members of the TGF-β superfamily. Phylogenetic analyses included the newly determined amino acid sequences of Nodal from *L. gigantea*, *B. glabrata* and *Capitella* sp. I, as well as the Nodal sequences of other deuterostomes and other TGF-β superfamily members available from GenBank. Sequence data were analysed with MacClade version 4.05 OSX, Clustal X version 1.62b, and PAUP* version 4.0b10. Gene orthology was determined by Bayesian-inference-based methods with MrBayes 3.12. Further details of phylogenetic analyses are available on request.

Sexually mature *L. gigantea* were collected in Los Angeles, California, during the breeding season, and *in vitro* fertilizations were performed as described previously[25]. A breeding population of *B. glabrata* is maintained in freshwater tanks at 25 °C, and embryos and larvae were regularly collected and raised in the laboratory. Embryos of both species were fixed as described previously[26]. PCR reactions were performed with gene-specific (for *L. gigantea*) and degenerate (for *B. glabrata*) primer sequences (available from the authors on request). 5′ and 3′ RACE PCR was performed with Invitrogen RACE reagents. *In situ* hybridizations were performed with digoxigenin- and fluorescein-labelled RNA probes as described previously[26]. Nodal inhibition was performed by placing egg masses of *B. glabrata* in fresh water containing 1% DMSO and SB-431542 (TOCRIS Bioscience) at concentrations of 5 µM or 10 µM (diluted from a 1 mM stock of SB-431542 in DMSO); treatment with rapamycin was performed by placing egg masses in fresh water containing 1% DMSO and rapamycin (Eton Bioscience Inc.) at 10 µM (diluted from a 10 mM stock of rapamycin in DMSO). Control embryos were exposed to 1% DMSO. All controls and drug-treated embryos were kept in the dark during the treatment period.

1. Massagué, J. & Gomis, R. R. The logic of TGFβ signaling. *FEBS Lett.* **580**, 2811–2820 (2006).
2. Hamada, H., Meno, C., Watanabe, D. & Saijoh, Y. Establishment of vertebrate left–right asymmetry. *Nature Rev. Genet.* **2**, 103–113 (2002).
3. Supp, D. M., Witte, D. P., Potter, S. S. & Brueckner, M. Mutation of an axonemal dynein affects left–right asymmetry in *inversus viscerum* mice. *Nature* **389**, 963–966 (1997).
4. Okada, Y. *et al.* Abnormal nodal flow precedes *situs inversus* in iv and inv mice. *Mol. Cell* **4**, 459–468 (1999).
5. Morokuma, J., Ueno, M., Kawanishi, H., Saiga, H. & Nishida, H. *HrNodal*, the ascidian nodal-related gene, is expressed in the left side of the epidermis, and lies upstream of *HrPitx*. *Dev. Genes Evol.* **212**, 439–446 (2002).
6. Duboc, V., Rottinger, E., Besnardeau, L. & Lepage, T. *Nodal* and *BMP2/4* signaling organizes the oral–aboral axis of the sea urchin embryo. *Dev. Cell* **6**, 397–410 (2004).
7. Duboc, V., Rottinger, E., Lapraz, F., Besnardeau, L. & Lepage, T. Left–right asymmetry in the sea urchin embryo is regulated by nodal signaling on the right side. *Dev. Cell* **9**, 147–158 (2005).
8. Schilthuizen, M. & Davison, A. The convoluted evolution of snail chirality. *Naturwissenschaften* **92**, 504–515 (2005).
9. Boycott, A. E. & Diver, C. On the inheritance of sinistrality in *Limnaea peregra. Proc. R. Soc. Lond. B* **95**, 207–213 (1923).
10. Sturtevant, A. H. Inheritance of direction of coiling in *Limnaea. Science* **58**, 269–270 (1923).
11. Freeman, G. & Lundelius, J. The developmental genetics of dextrality and sinistrality in the gastropod *Lymnaea peregra. Wilhelm Roux Arch. Dev. Biol.* **191**, 69–83 (1982).
12. Nederbragt, A. J., van Loon, A. E. & Dictus, W. J. Evolutionary biology: *hedgehog* crosses the snail's midline. *Nature* **417**, 811–812 (2002).
13. van den Biggelaar, J. A. M., van Loon, A. E. & Damen, W. G. M. Mesentoblast and trochoblast specification in species with spiral cleavage predict their phyletic relations. *Neth. J. Zool.* **46**, 8–21 (1995).
14. Lartillot, N., Lespinet, O., Vervoort, M. & Adoutte, A. Expression pattern of *Brachyury* in the mollusc *Patella vulgata* suggests a conserved role in the establishment of the AP axis in Bilateria. *Development* **129**, 1411–1421 (2002).

15. Dictus, W. J. A. G. & Damen, P. Cell lineage and clonal-contribution map of the trochophore larva of *Patella vulgata* (Mollusca). *Mech. Dev.* 62, 213–226 (1997).

16. Inman, G. J. *et al.* SB-431542 is a potent and specific inhibitor of transforming growth factor-β superfamily type I activin receptor-like kinase (ALK) receptors ALK4, ALK5, and ALK7. *Mol. Pharmacol.* 62, 65–74 (2002).

17. Christiaen, L. *et al.* Evolutionary modification of mouth position in deuterostomes. *Semin. Cell Dev. Biol.* 18, 502–511 (2007).

18. Nogi, T., Yuan, Y. E., Sorocco, D., Perez-Tomas, R. & Levin, M. Eye regeneration assay reveals an invariant functional left–right asymmetry in the early bilaterian, *Dugesia japonica. Laterality* 10, 193–205 (2005).

19. Oviedo, N. J. & Levin, M. Gap junctions provide new links in left–right patterning. *Cell* 129, 645–647 (2007).

20. Ponder, W. F. & Lindberg, D. R. Towards a phylogeny of gastropod molluscs: analysis using morphological characters. *Zool. J. Linn. Soc.* 119, 83–265 (1997).

21. Hibino, T., Nishino, A. & Amemiya, S. Phylogenetic correspondence of the body axes in bilaterians is revealed by the right-sided expression of *Pitx* genes in echinoderm larvae. *Dev. Growth Differ.* 48, 587–595 (2006).

22. Palmer, A. R. Symmetry breaking and the evolution of development. *Science* 306, 828–833 (2004).

23. Duboc, V. & Lepage, T. A conserved role for the Nodal signaling pathway in the establishment of dorso–ventral and left–right axes in deuterostomes. *J. Exp. Zool. B Mol. Dev. Evol.* 310, 41–53 (2008).

24. Levin, M. Left–right asymmetry in embryonic development: a comprehensive review. *Mech. Dev.* 122, 3–25 (2005).

25. Gould, M. C., Stephano, J. L., Ortíz-Barrón, B. J. & Pérez-Quezada, I. Maturation and fertilization in *Lottia gigantea* oocytes: intracellular pH, Ca^{2+}, and electrophysiology. *J. Exp. Zool.* 290, 411–420 (2001).

26. Price, A. L. & Patel, N. H. Investigating divergent mechanisms of mesoderm development in arthropods: the expression of *Ph-twist* and *Ph-mef 2* in *Parhyale hawaiensis. J. Exp. Zoolog. B Mol. Dev. Evol.* 310, 24–40 (2008).

27. Shibazaki, Y., Shimuzu, M. & Kuroda, R. Body handedness is directed by genetically determined cytoskeletal dynamics in the early embryo. *Curr. Biol.* 14, 1462–1467 (2004).

28. Camey, T. & Verdonk, N. H. The early development of the snail *Biomphalaria glabrata* (Say) and the origin of the head organs. *Neth. J. Zool.* 20, 93–121 (1970).